Polymer Films on Electrodes. 30. Electrochemistry and Scanning Electrochemical Microscopy Characterization of Benzimidazolebenzophenanthroline-Type Ladder (BBL) and Semiladder (BBB) Polymer Films

Maurizio Quinto,[†,‡] Samson A. Jenekhe,[§,¶] and Allen J. Bard*[,†]

Department of Chemistry and Biochemistry, The University of Texas at Austin, Austin, Texas 78712 and Department of Chemical Engineering, University of Rochester, Rochester, New York 14627

Received December 29, 2000. Revised Manuscript Received June 11, 2001

Polymer-modified electrodes were obtained by spin-coating solutions of poly(benzobisimidazobenzophenanthroline) ladder (BBL) and semiladder (BBB) polymers on indium−tin oxide electrodes. An electrochemical study of these films showed reproducible and stable cyclic voltammograms for reduction of the polymer (in the absence of oxygen), the absence of waves for oxidation of the polymer, and brilliant changes in color during the potential scan. Measurements with the scanning electrochemical microscope showed changes in the film conductivity, with the films being more conductive in the reduced form. The potential dependence of the film resistance and atomic force microscopic characterization are also reported. These results confirm the electron transport and electron-accepting nature of both BBL and BBB, which can accept up to two electrons per monomer repeat unit. Although the electrochromic features of BBL and BBB are similar, a significant difference in the film morphologies was observed by atomic force microscopy.

Introduction

In the class of organic polymers as a whole, ladder-type polymers exhibit many remarkable properties,[1−9] and a systematic study of their electronic and spectroscopic behavior is of interest. The poly[6,9-dihydro-6,9-dioxobisbenzimidazo[2,1-*b*:1′,2′- *j*]benzo[1mn]phenanthroline-2,12-diyl] (BBB) and poly[17-oxo-7,10-benz[de]-imidazo[4′,5′:5,6]-benzimidazo[2,1-a]isoquinoline-3,4:10,11-tetrayl)-10-carbonyl]) (BBL) materials (Figure 1) are members of a broad class of thermally stable rigid-chain polymers.[2−9] They generally contain aromatic or heterocyclic rings together with other groups that promote strong primary and van der Waals bonding forces, resonance stabilization, and molecular symmetry, which make them very robust materials.[2−9] BBB and BBL polymers, which are the primary focus here, are made by polycondensations of 1,4,5,8-naphthalene-tetracarboxylic acid with 3,3-diaminobenzidine and 1,2,4,5-tetraaminobenzene, respectively.[2,3]

In general, these rigid-chain polymers, which show desirable physicochemical properties such as high-temperature resistance, are difficult to process because of their insolubility in organic solvents and high glass transition, softening, or melting temperatures (>250−300 °C).[2−9] Jenekhe and Johnson[8a] used a reversible electron donor−acceptor complex formation between heterocyclic polymers and Lewis acids to solubilize these polymers in aprotic organic solvents. In this work, a metal halide Lewis acid, $GaCl_3$, was used to solubilize and process rigid-chain polymers, including ladder polymers such as BBL and semiladders such as BBB.[8,9] This complexation involves coordination of the Lewis acid to the electron-rich carbonyl oxygen and the imine nitrogen in the polymer backbone. The resulting solutions of the BBB or BBL complex can then be processed into films by methods such as solvent casting or spin coating.[8,9]

BBL probably has a delocalized electronic structure and, upon doping, forms an electronically conducting polymer.[10−13] It can be chemically[10] or electrochemi-

† The University of Texas at Austin.
‡ Current address: Università di Foggia, Facoltà di Agraria, via Napoli 25, 71100 Foggia, Italy.
§ University of Rochester.
¶ Current address: Department of Chemical Engineering, University of Washington, Seattle, WA 98195-1750.

(1) Schluter, A. D. *Adv. Mater.* **1991**, *3*, 282.
(2) Van Deusen, R. L. *J. Polym. Sci., Polym. Lett.* **1966**, *4*, 211.
(3) (a) Van Deusen, R. L.; Goins, O. K.; Sicree, A. J. *J. Polym. Sci. A-1* **1968**, *6*, 1777. (b) Arnold, F. E.; Van Deusen, R. L. *Macromolecules* **1969**, *2*, 497.
(4) Frazer, A. H. *High Temperature Resistant Polymers*; Wiley-Interscience: New York, 1968.
(5) Cassidy, P. E. *Thermally Stable Polymers*; Marcel Dekker: New York, 1980.
(6) Critchley, J. P.; Knight, G. J.; Wright, W. W. *Heat-Resistant Polymers*; Plenum: New York, 1983.
(7) Hergenrother, P. M. In *Encyclopedia of Polymer Science and Engineering*; Korschwitz, J. I., Ed.; Wiley: New York, 1985; Vol. 7, pp 639−665.
(8) (a) Jenekhe, S. A.; Johnson, P. O. *Macromolecules* **1990**, *23*, 4419. (b) Roberts, M. F.; Jenekhe, S. A *Polymer* **1994**, *35*, 4313.
(9) Roberts, M. F.; Jenekhe, S. A *J. Polym. Sci., Part B: Polym. Phys.* **1995**, *33*, 577.
(10) (a) Kim, O.-K. *J. Polym. Sci., Polym. Lett. Ed.* **1982**, 663. (b) Kim, O.-K. *Mol. Cryst. Liq. Cryst.* **1984**, *105*, 161.
(11) (a) Narayan, K. S.; Alagiriswamy, A. A.; Spry, R. J. *Phys. Rev. B.* **1999**, *59*, 10054. (b) Antoniadis, H.; Abkowitz, M. A.; Osaheni, J. A.; Jenekhe, S. A.; Stolka, M. *Chem. Mater.* **1994**, *6*, 63.

10.1021/cm001426f CCC: $20.00
Published on Web 08/10/2001

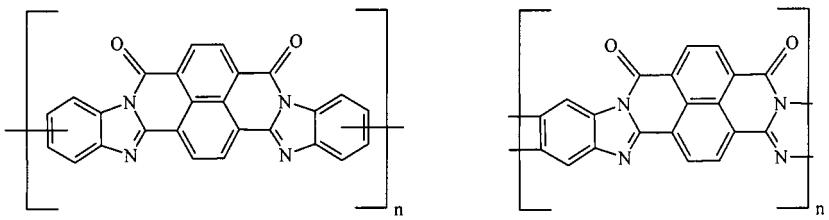

Figure 1. Structures of rigid-chain conjugated polymers BBB (left) and BBL (right).

cally[11] doped. Pristine BBL and BBB are both insulators with conductivities in the range of 10^{-14} S cm^{-1}.[11] The direct current conductivity of their films can be varied across a wide range by either ion implantation ($\geq 10^2$ S cm^{-1}) or thermal treatment.[11,12] This polymer also shows interesting mechanical properties and thermal stability[14] because of its ladder structure. BBL forms liquid crystalline solutions owing to its rodlike extended chain structure.[8b] BBB, in contrast to BBL, is a linear polymer that does not form liquid crystalline mesophases in solution.[8] A scanning tunneling microscopy (STM) study of BBB films shows structural features that include helical fibers coiled into strands, with the strands coiled into strings.[15]

Recent interest in BBL films has focused on its intrinsic semiconducting,[11,16] photoconductive,[17] and nonlinear optical[18] properties together with optoelectronic device applications.[19] This conjugated ladder polymer has an optically determined semiconductor band gap of 1.8 eV. Photovoltaic cells based on BBL thin films were recently demonstrated,[19a] showing very high charge collection efficiencies (49%) and power conversion efficiencies of up to 2%. Photodetectors with ultralow dark currents (<1 nA), broad visible-near-infrared photoresponse, and high photosensitivity have been made from BBL thin-film nanocomposites with metallophthalocyanines.[19b] However, when BBL was used as an electron transport layer in poly(*p*-phenylenevinylene)-based light-emitting diodes the electroluminescence was completely quenched because of photoinduced charge transfer and separation in the heterojunctions.[19c]

To understand better the characteristics of BBL and BBB films and to correlate their redox properties and spectroscopic behavior with macromolecular structure, a detailed electrochemical study was performed. We also determined the resistance dependence on the applied electrode potential. The results obtained for the BBL film are in accordance with previous experiments,[20] which investigated the voltammetric behavior, conductivity characteristics, and spectroelectrochemistry of the BBL polymer spread on Pt and glassy carbon disks in both aqueous and acetonitrile solutions.[20a,b]

In the work reported here, the surface topography and the BBB and BBL film thicknesses were studied by atomic force microscopy (AFM). Electrochemical reduction and oxidation (doping and undoping) processes of BBB and BBL in 0.1 tetra-*n*-butylammonium hexafluorophosphate ($TBAPF_6$) acetonitrile solution were studied by scanning electrochemical microscopy (SECM) to characterize the electron transfer of polymers with a redox mediator in solution at different levels of reduction. These measurements allowed a study of the film conductivity and a calculation of an apparent heterogeneous rate constant for charge transport.

Experimental Section

The synthesis of the polymers and their solubilization and film processing in aprotic organic solvents are described elsewhere.[2,3,8,9] We used a BBL sample with an intrinsic viscosity of 32 dL/g in methanesulfonic acid at 30 °C; the BBB sample had an intrinsic viscosity of 3.7 dL/g under similar conditions.[8,9,16] Solutions of BBL or BBB in nitromethane/$GaCl_3$ were 0.1−0.2 wt. % polymer.

The thin films were prepared on an ITO surface (resistance, 30−60 ohm/square; Delta Technologies, Stillwater, MN) by spin-coating 0.2 mL of solution onto a 1 cm^2 ITO surface at 2000 rpm for 30 s. This procedure led to the production of very thin films (20−40 nm). The polymer films were then put into a deionized water bath for 8 h to remove $GaCl_3$. Finally, the films were dried in a vacuum chamber at 40 °C for 6 h. The connection to the ITO was made by sealing a metal wire in a polymer-free zone of the ITO surface with silver epoxy glue.

$TBAPF_6$ (SACHEM, Austin, TX) was recrystallized from $EtOH/H_2O$ (4:1) twice and dried at 100 °C before use. Acetonitrile (Burdick and Jackson, UV grade) was used as received after being transported unopened into an inert atmosphere drybox.

Electrochemistry experiments were conducted with a CHI 660 electrochemical workstation (CH Instruments, Austin, TX) with use of a three-electrode cell. Unless specified otherwise, care was taken to avoid the introduction of any oxygen and water into the cell by preparing the electrolyte solution in a drybox (Vacuum Atmospheres) and using a sealed cell, which did not permit contact of the solution and the electrodes with the atmosphere.

The electrolyte solution was a MeCN solution with 0.1 M $TBAPF_6$ supporting electrolyte. The polymer is insoluble in MeCN, so the polymer film remained intact across a broad range of potentials during the electrochemical experiments. A platinum coil was used as the counter electrode, and a silver wire was used as a quasireference electrode, which was calibrated vs SCE by the addition of ferrocene as an internal standard using $E°$ (Fc/Fc^+) = 0.424 vs SCE.

(12) (a) Jenekhe, S. A.; Tibbetts, S. J. *J. Polym. Sci., Part B: Polym. Phys.* **1988**, *26*, 201. (b) Long, V. C.; Washburn, S.; Chen, X. L.; Jenekhe, S. A. *J. Appl. Phys.* **1996**, *80*, 4202.

(13) (a) Polyak, L.; Rollison, D. R.; Kessler, R. J.; Nowak, R. Abstract of Papers, 163rd Meeting of the Electrochemical Society, May 1983: Extended Abstract 547; The Electrochemical Society: Princeton, NJ. (b) Jenekhe, S. A. *Polym. Mater. Sci. Eng.* **1989**, *60*, 419.

(14) Powell, J. W.; Chartoff, R. P. *J. Appl. Polym. Sci.* **1974**, *13*, 83.

(15) Munz, A. W.; Schmeisser, D.; Gopel, W. *Chem. Mater.* **1994**, *6*, 2288.

(16) Chen, X. L.; Jenekhe, S. A. *Macromolecules* **1997**, *30*, 1728.

(17) (a) Osaheni, J. A.; Jenekhe, S. A.; Perlstein, J. *J. Phys. Chem.* **1994**, *98*, 12727. (b) Antoniadis, H.; Abkowitz, M. A.; Osaheni, J. A.; Jenekhe, S. A.; Stolka, M. *Synth. Met.* **1993**, *60*, 149.

(18) Jenekhe, S. A.; Roberts, M. F.; Agrawal, A. K.; Meth, J. S.; Vanherzeele, H. *Mater. Res. Soc. Proc.* **1991**, *214*, 55.

(19) (a) Jenekhe, S. A.; Yi, S. *Appl. Phys. Lett.* **2000**, 77, 2635. (b) Jenekhe, S. A.; Yi, S. *Adv. Mater.* **2000**, 12, 1274. (c) Zhang, X.; Jenekhe, S. A. *Macromolecules* **2000**, *33*, 2069.

(20) (a) Wilbourn K.; Murray R. W. *J. Phys. Chem.* **1988**, *92*, 3642. (b) Wilbourn K.; Murray R. W. *Macromolecules* **1988**, *21*, 89. (c) Yohannes, T.; Neugebauer, H.; Luzzati, S.; Catellani, M.; Jenekhe, S. A.; Sariciftci, N. S. *J. Phys. Chem. B* **2000**, *104*, 9430.

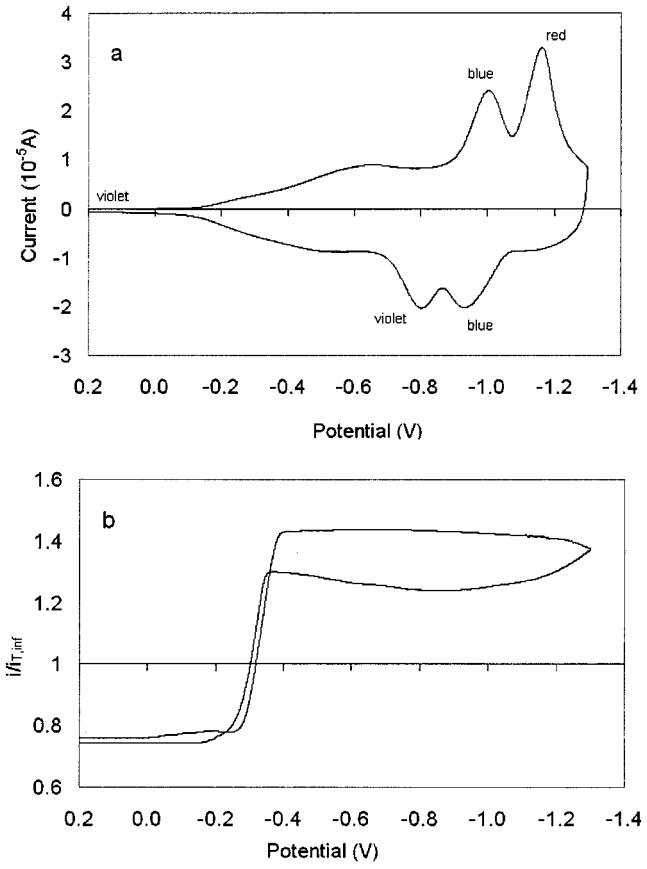

Figure 2. (a) Cyclic voltammetry of a BBL thin film spin-coated on an ITO electrode (surface area, 1 mm^2) in MeCN, 0.1 M $TBAPF_6$. The color of the film changed as indicated. (b) Tip current, i_T, recorded during the potential scan (scan rate, 20 mV/s). The tip was positioned by maintaining the film in the conductive state and recording an approach curve until $i_T/i_{T,\infty} = 1.25$.

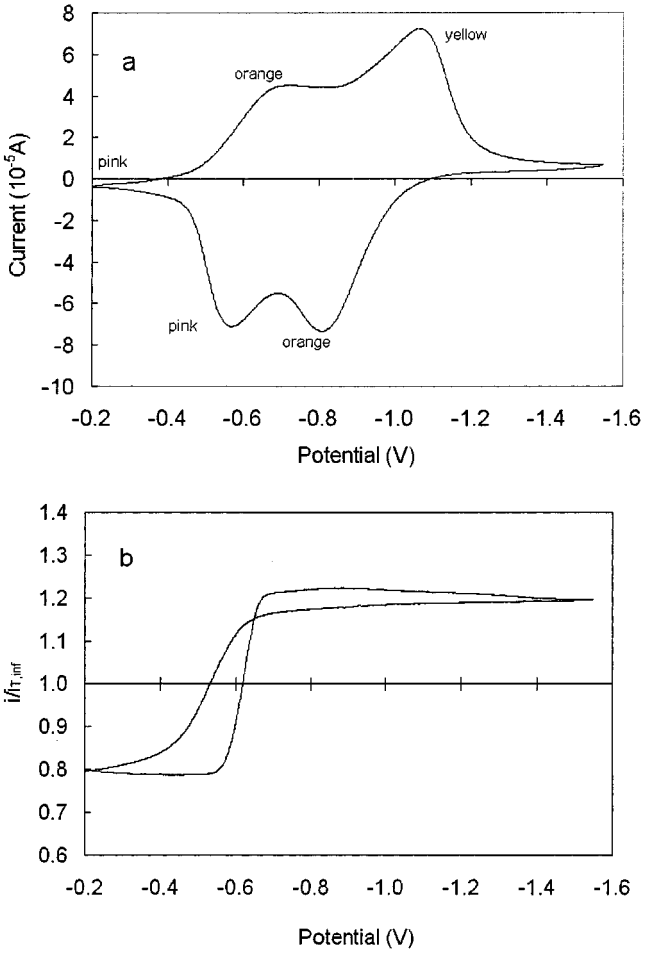

Figure 3. (a) Cyclic voltammetry of a BBB thin film spin-coated on an ITO electrode (surface area, 3 mm^2) in MeCN, 0.1 M $TBAPF_6$. The color of the film changed as indicated. (b) Tip current, i_T, recorded during the potential scan. Same experimental conditions as in Figure 2.

UV−vis spectra were recorded on a Milton Roy Spectronic 3000 array spectrophotometer. The background subtraction was obtained with the same cell as that used for the spectroelectrochemical experiments, with an untreated ITO as the working electrode.

Imaging experiments were performed with a Nanoscope II (Digital Instruments, Santa Barbara, CA) AFM in air at room temperature and atmospheric pressure. The images were not digitally filtered. The sample was manually positioned below the tip and maintained perpendicular to the sample surface through the microscope adjustment screws. In the study to determine the film thickness with AFM, part of the film was removed from the ITO surface with a razor blade.

The experimental setup for SECM measurements has been described previously.[21] Potentiostatic experiments of the polymer-covered substrate were performed with tetrathiafulvalene (TTF) as mediator. Cyclic voltammetry with this compound showed that at a potential of 0.2 V applied to the tip for the approach curve experiments, the electrode reaction is diffusion controlled. The tip was positioned close to the polymer film in the conductive state ($E_{sub} = 1.1$ V) and was stopped when $i_T/i_{T,\infty} = 1.25$. The electrolyte solution was 0.1 M $TBAPF_6$ in MeCN, and the concentration of the mediator was 5 mM. The solutions were bubbled with Ar before the SECM experiments; and during the measurements, the cell was maintained under an Ar atmosphere. The CHI 660 electrochemical workstation was used for the tip characterization in the absence of the polymer substrate.

Resistance measurements in solution were performed as described previously.[22] This method used a four-microband-electrode array covered by the film (obtained by dip coating). The resistance measurement was performed with a dc voltmeter connected between the two central microbands, whereas the potential applied to the external microbands was varied.

Results

Cyclic Voltammetry. Cyclic voltammograms for an electrode coated with a BBL film spin-coated onto an ITO surface (Figure 2a) showed three fairly well-defined reduction waves. Different reduction potential limits were chosen during the cyclic voltammograms, showing the relation between the reduction and the relevant oxidation waves. Brilliant changes in the film color were clearly visible during the scans. The second reduction process caused the initially violet film to become blue, whereas the third reduction changed the color of the film to red. These electrochromic effects were stable and reversible under anaerobic and anhydrous conditions; the film continued to exhibit strong color changes after more than 500 successive cycles in MeCN.

Figure 3a shows a cyclic voltammogram for a BBB spin-coated film on ITO. In this case, two different

(21) Wipf, D.; Bard, A. J. *J. Electroanal. Chem.* **1991**, *138*, 489.

(22) Quinto, M.; Bard, A. J. *J. Electroanal. Chem.* **2001**, *498*, 67.

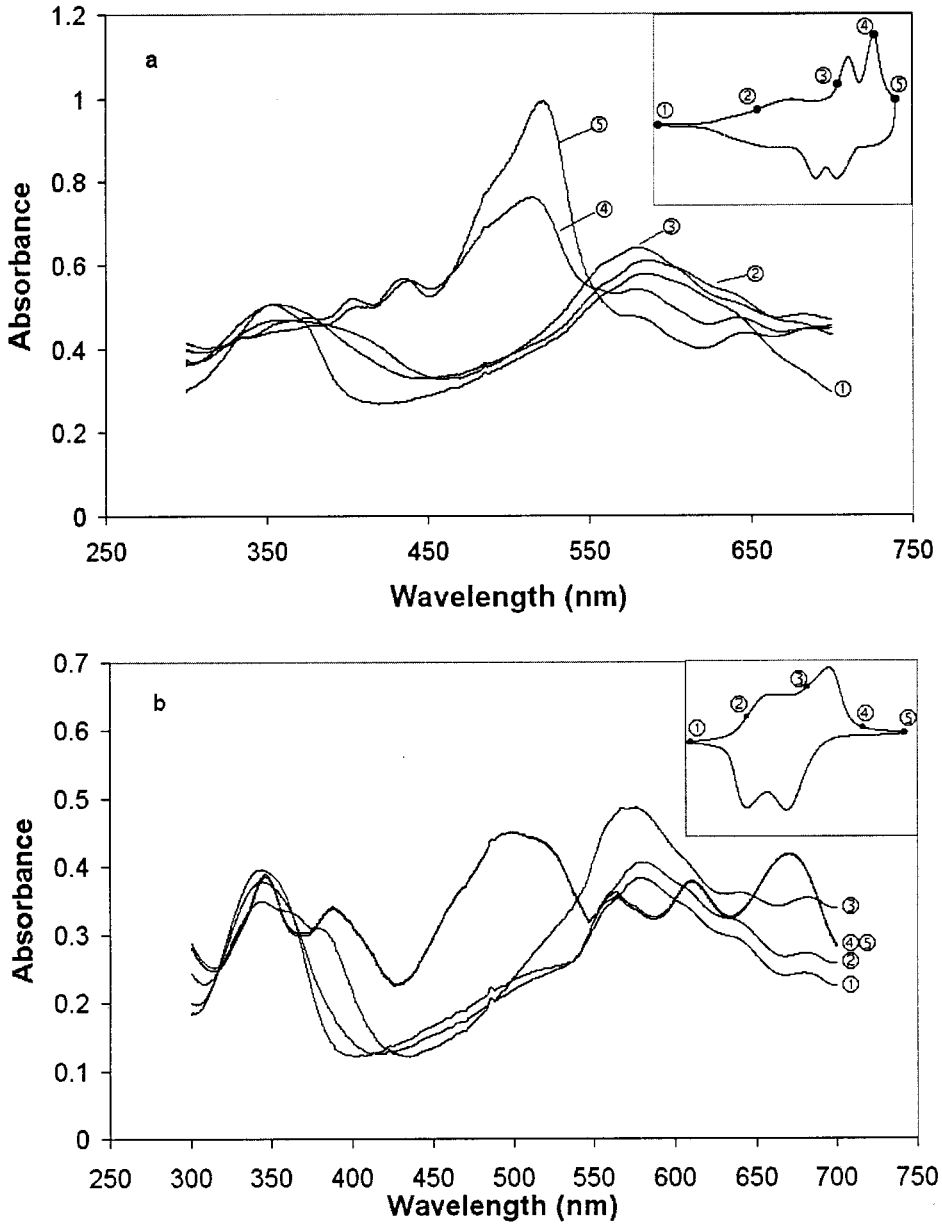

Figure 4. Absorption spectra at different potentials of (a) BBL and (b) BBB thin films on ITO in MeCN, 0.1 M $TBAPF_6$. Insets show the potentials at which spectra were obtained.

reduction peaks are clearly visible; each correlates with the corresponding oxidation peaks in the reverse scan. As reported in Figure 2a, changes in the film color are clearly visible during the scans and correlate to the different film reduction states.

Under these conditions, no electrochemical activity was recorded for both films in the zone between 0 and 2.0 V, indicating that the films are not oxidized in this potential range. More positive potentials cause solvent oxidation.

Electronic absorption spectra of BBB and BBL films were obtained by applying different potentials (Figure 4). The spectral traces are taken at potentials that span the voltammetric waves shown in Figures 2a and 3a. BBL spectra showed an increase and decrease in absorbance at 524 and 583 nm, respectively, and two not very well-defined isosbestic points at 375 and 550 nm. BBB spectra did not show clear isosbestic points. For the most reduced form, the maximum peak is at 503 nm, and as the applied potential passed over the first voltammetric feature, the film exhibited a peak at 576 nm.

Atomic Force Microscopy. An AFM study was performed for imaging the film surface and determination of the thickness of the films. The topography of the BBL film (Figure 5a) showed a rough surface with clusters 50−100 nm in diameter. This study revealed an average thickness of 25 nm with a standard deviation (RMS) of 3.0 nm.

The BBB film (Figure 5b) appeared less rough than the BBL film, and it is possible to recognize a structure of well-organized parallel rows, probably because of interpolymer chain interactions. The BBB film showed an average thickness of 35 nm with a standard deviation (RMS) of 2.4 nm.

Film Resistivity. The film conductivity properties in solution have been investigated by SECM measuring the feedback current when the tip was brought close to the polymer-modified electrodes (Figure 6). Potentiostatic experiments and cyclic voltammetry of the polymer-

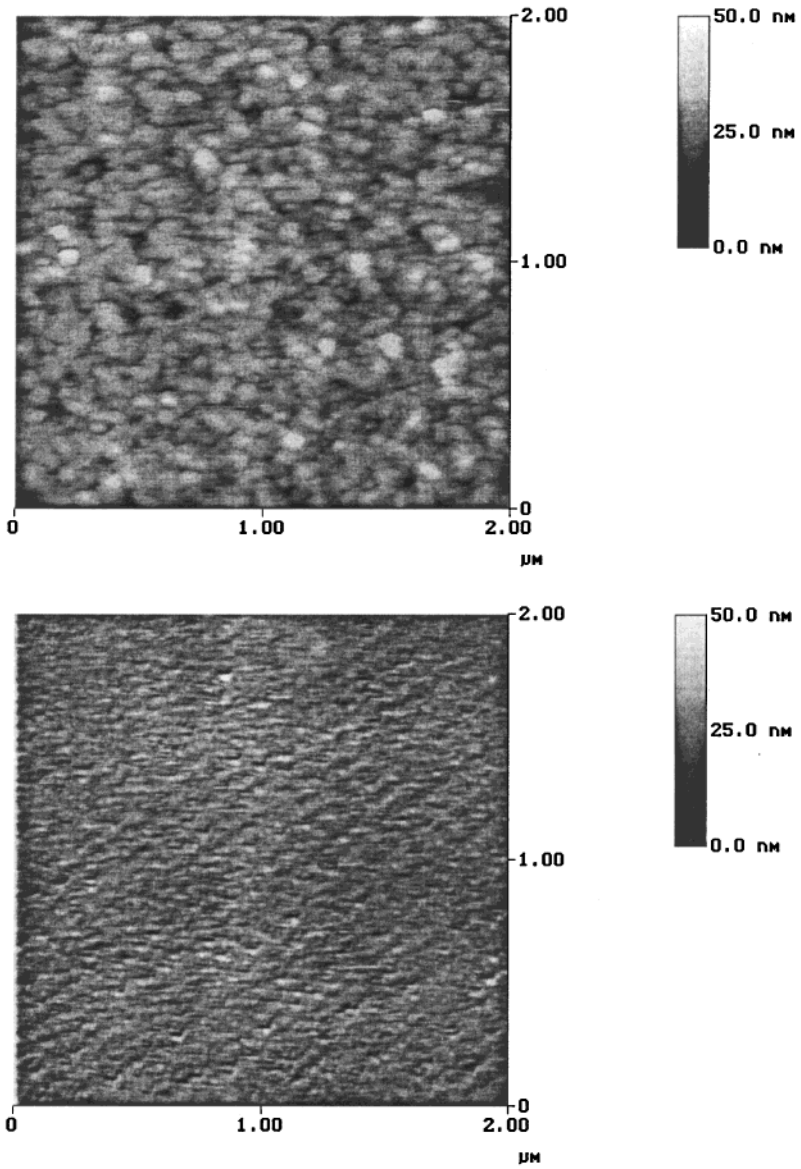

Figure 5. AFM images of (a) BBL and (b) BBB films deposited by spin-coating (2000 rpm, 30 s). The film thicknesses are (a) ~25 nm and (b) ~35 nm under these conditions (thicknesses obtained by AFM measurements).

covered substrates were performed with a mediator when the tip was close to the substrate to study the electron transfer at the BBL and BBB (Figures 2b and 3b). The tip current (i_T) is caused by the electrochemical oxidation of TTF to $TTF^{\bullet+}$ with the tip potential, E_T, biased at +0.2 V. The feedback current indicates the extent of tip-generated $TTF^{\bullet+}$ reduction back to TTF on the polymer film. For both films, the unreduced state showed SECM approach curves characteristic of insulators (negative feedback). Positive feedback approach curves appeared on film reduction, signaling reduction of $TTF^{\bullet+}$ on reaction with reduced surface forms and conduction of electrons through the film.

To investigate the film permeability in their neutral forms, cyclic voltammograms with the mediator (TTF) in solution were taken at the ITO electrode before and after the spin coating (Figure 7). The presence of the film decreased the peak height and increased the peak splitting. However, for both films the behavior is characteristic of pinholes in the films allowing some direct access of solution TTF to the ITO substrate.

To study the film conductivity and its changes with potential, direct resistance measurements during cyclic voltammetry were performed with an array of four Pt microbands (1 mm long, 25 μm wide, and 25 μm apart) following the basic procedure used previously.[22] The film deposition was effected by dip coating. The measurements shown in Figure 8 demonstrate that the neutral forms of the BBB and BBL films are always much less conductive than the reduced forms and generally show the same increase in conductivity upon reduction that is found in the SECM scans.

Discussion

A linear dependence of peak current density on scan rate (v) with a zero intercept was observed for the BBL and BBB films at low scan rates (v = 50 mV/s), providing evidence that the electrochemical reactions occur within the thin film on the electrode surface and not in solution. At lower scan rates, the amount of the charge involved in the overall reduction process was constant and essentially equal to the charge recorded

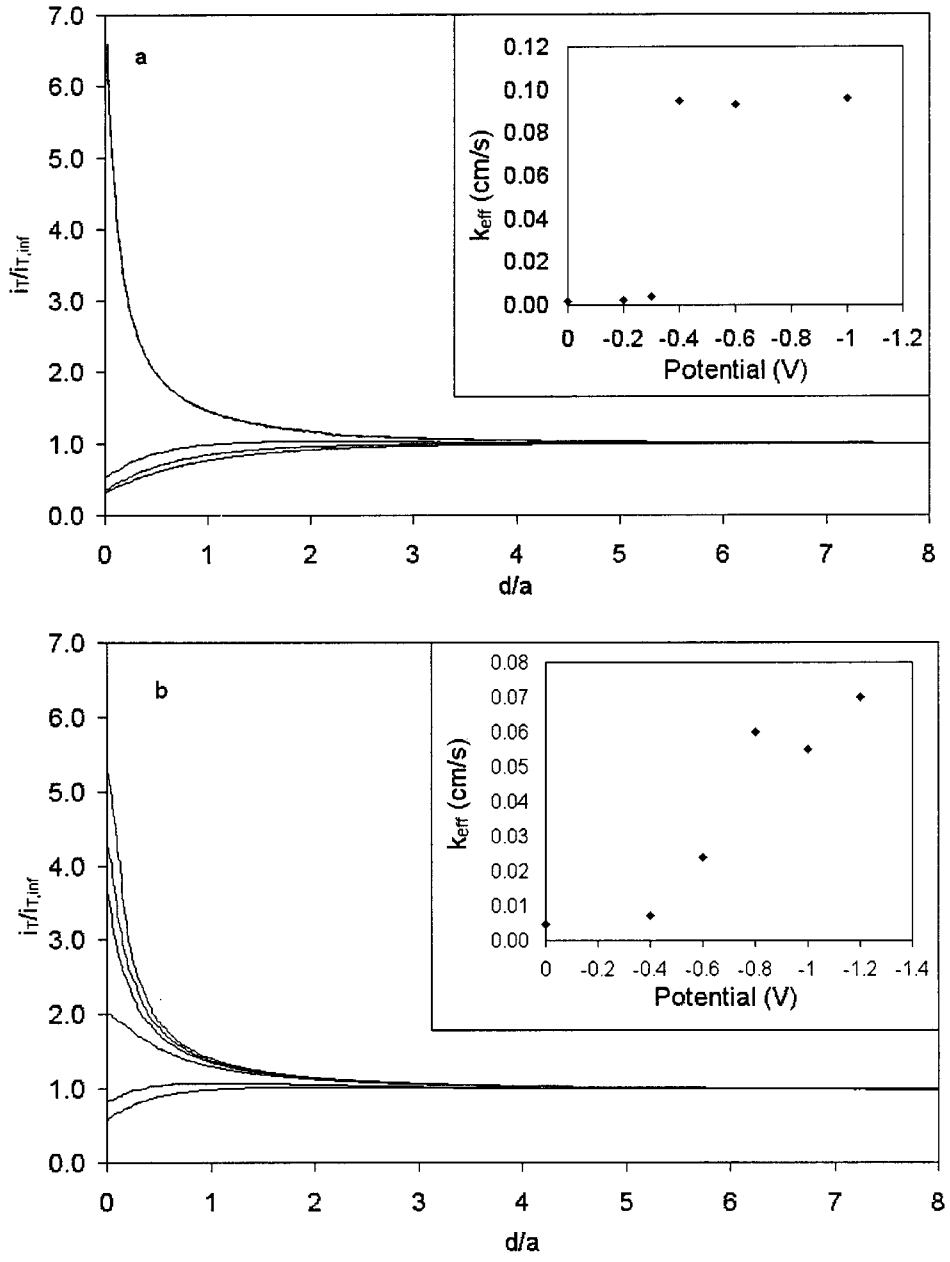

Figure 6. SECM tip (a = 12.5 μm) approach curves with 5 mM TTF as redox mediator on (a) BBL and (b) BBB at different potentials. Potentials are from bottom to top: (a) 0.0, −0.2, −0.3, −0.4, −0.6, −0.8 V (last three curves are superimposed) and (b) 0.0, −0.4, −0.6, −0.8, −1.0, −1.2 V. Insets: Variation of k_{eff} with the potential applied to the film.

in the oxidation process. At faster scan rates, the i_p/v value decreased, suggesting the onset of kinetic limitations.

Considering that (a) the thickness of the film obtained by AFM measurements (25 ± 3 nm for BBL and 35 ± 2 nm for BBB); (b) the surface area of the modified electrode (0.092 ± 0.001 cm^2 for BBL and 0.096 ± 0.001 cm^2 for BBB); and (c) the volume occupied by a single monomer unit estimated by a computer simulation of the molecular structure (0.144 ± 0.003 nm^3 for BBL and 0.165 ± 0.003 nm^3 for BBB), we can make a rough estimate of the number of monomer units per electrode ($1.6 \pm 0.2 \cdot 10^{15}$ for BBL and $2.0 \pm 0.2 \cdot 10^{15}$ for BBB). The theoretical charge for a one-electron process for the polymer films is then 260 ± 30 μC for the BBL film and 320 ± 30 μC for the BBB films. From the cyclic voltammetry, the total charge involved in the cathodic processes was 537 μC for the BBL and 625 μC for the BBB film. These results show that during the first and the second reductions, the electron/monomer ratio is close to two for both polymers. In other words, the polymers accept on average up to two electrons per monomer site during the overall reduction, and the process involves the entire film structure. At faster scan rates, the overall charge amount diminishes, and a linear dependence of current versus the square root of the scan rate was noted. In particular, slopes obtained for the reduction processes were comparable, and similar results were found for the oxidation processes. These results suggest that the rate of the electrode process is now being governed by one that can be taken as a diffusional one. Processes that govern the current under these conditions can be complex,[23] because electron hopping through the film and movement of the electrolyte species into the film during the redox processes are coupled. For example, cation diffusion into the film is

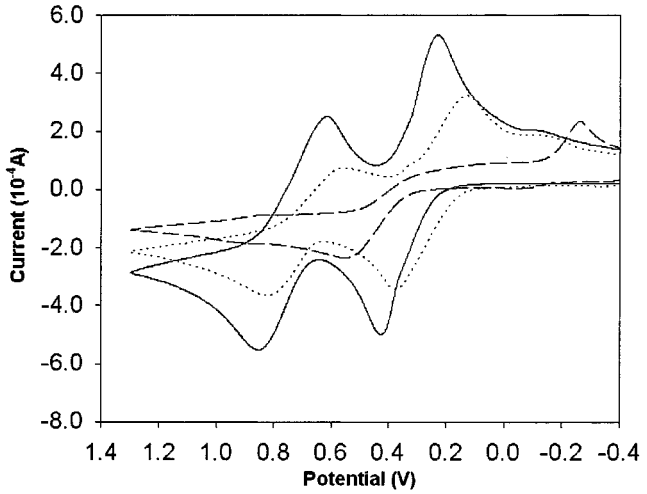

Figure 7. Cyclic voltammograms of 5 mM TTF in MeCN, 0.1 M $TBAPF_6$, on a bare ITO electrode (solid line), BBL-coated ITO electrode (dotted line), and BBB-coated ITO electrode (dashed line).

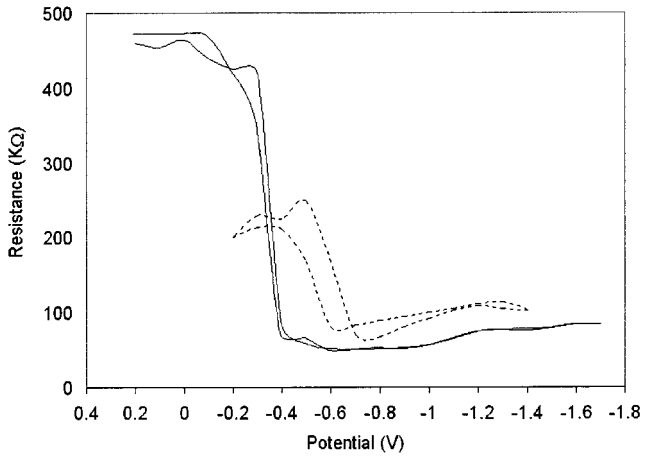

Figure 8. Resistance dependence of BBL (solid line) and BBB (dotted line) films during cyclic voltammetry. Experimental conditions as in Figure 2, except scan rate was 10 mV/s. The resistance was measured between the central microbands, whereas the potential was applied to the external microbands.

one of the processes occurring during the reduction. If this, cation diffusion becomes the rds of the process, the slope of the $I - v^{1/2}$ curve would be proportional to the diffusion constant of cation in the film. The slow diffusion of cation into the film would not permit the complete reduction of the film during the scan, as demonstrated by a decrease of the charge and by the diminution of the color changes during the cyclic voltammetry. During reoxidation, cations leave the film and anions can diffuse in. These processes also become rate-determining at faster scan rates during anodic sweeps.

Changes in coloration during cyclic voltammetry can be followed by spectroelectrochemistry with optically transparent ITO electrodes equilibrated at various potentials. The presence of an isosbestic point is usually consistent with predominance of a single overall chemical reaction, proceeding from an oxidized state to a reduced product with one additional electron and cation. Even with BBL, the presence of isosbestic points denotes that the two reduction steps occur in the same redox center, most probably delocalized over several centers. In the BBB case, the absence of an isosbestic point suggests the presence of two different redox reactions in different redox polymer zones. This difference can be attributed to the different chain structures of the polymer ladder for BBL and semiladder for BBB.

The electrolysis of a species in solution at an electrode covered by an insulating film usually differs from that at a bare electrode. These differences depend on the extent of coverage of the electrode by the film, the size and distribution of pores or pinholes, and the time scale of the experiment. The theory for electrodes of this type is closely related to that for ultramicroelectrode arrays,[24] which, however, often involve a better-defined geometry and uniform distribution of active sites.[25,26] Several factors govern the shape of the cyclic voltammogram compared with that at the bare electrode.[27] The larger effects of heterogeneous electron-transfer kinetics are caused by a higher current density at the active sites. When individual sites behave as ultramicroelectrodes and are spaced apart at a sufficient distance that their diffusion layers do not overlap during the time of the scan, the voltammogram will represent that of a collection of ultramicroelectrodes and produce a steady-state voltammogram (i.e., a flat limiting current plateau rather than a typical CV peak). The different behavior of the BBL and BBB films is seen in the curves of Figure 7. The cyclic voltammogram of the BBL film shows a behavior similar to an array of microelectrodes, whereas that of the BBB film suggests the presence of larger pores. The high covered/uncovered peak height ratio can be explained by the fact that at slow sweep rates the diffusion layers from the individual sites grow together, overlap, and merge, so that the electrode behavior approaches that of the unfilmed electrode with a total area of that of the bare electrode.

These results agree with the AFM study (Figure 5), which reveals different film morphologies for BBL and BBB. The BBL AFM image shows a rough surface with clusters of 40 ± 15 nm. This cluster size is of the order of the average thickness of the film, 35 nm, so the presence of interparticle pores or pinholes is reasonable. The BBB film shows a different image. A well-ordered and defined structure appears, with small imperfections that can cause the presence of channels in the film with dimensions of the order of microelectrodes. The presence of pores in the BBB and BBL structure was also noticed during SECM experiments. In a few cases, in the presence of a pore, the current measured during an approach curve revealed positive feedback (not shown) because the tip was approaching the uncovered ITO substrate.

Previous papers[22,28,29] described the application of the SECM technique in the study of the transition between the insulating and conductive states of electronically

(23) (a) Andrieux, C. P.; Savéant, J. M. *J. Phys. Chem.* **1988**, *92*, 6761. (b) Majda, M. In *Molecular Design of Electrode Surfaces*; Murray, R. M., Ed.; Wiley: New York, 1992; Chapter 4, pp 159−206.

(24) Leddy, J.; Bard A. J. *J. Electroanal. Chem.* **1983**, *153*, 223.
(25) Scharifker, B. R. *J. Electroanal. Chem.* **1988**, *230*, 61.
(26) Reller, H.; Kirowa-Einser, E.; Gileadi, E. *J. Electroanal. Chem.* **1982**, *138*, 65.
(27) Amatore, C.; Saveant, J.-M.; Tessier, D. *J. Electroanal. Chem.* **1983**, *147*, 39.
(28) Tsionsky, M.; Bard, A. J.; Dini, D.; Decker, F. *Chem. Mater.* **1998**, *10*, 2120.
(29) Kwak, J.; Lee, C.; Bard, A. J. *J. Electrochem. Soc.* **1990**, *5*, 1481.

conducting polymers. In general, conductive polymers allowed the regeneration of a mediator species produced at a tip (positive feedback) held near the polymer/solution interface, whereas a nonconductive film produced negative feedback, i.e., a decrease in the tip current as it approached the film/solution interface. To observe negative feedback, it is also necessary that the film is not permeable to the redox species generated at the tip. A small, but finite, film permeability results in a different approach curve with less pronounced negative feedback than that obtained with an insulating substrate.

The SECM behavior of the film can be rationalized by a previously proposed model.[28] The current across the film/solution interface in an SECM experiment,[30] as measured by the feedback current at the tip, is affected by four factors. These are diffusion of the mediator between the tip and polymer surface, electron transfer (ET) at the polymer/liquid interface, charge transport across the polymer film, and ET between the underlying metal and the polymer film. In an approach similar to the treatment of ET across a liquid/liquid interface,[31,32] one can treat the rates of several processes that occur in a serial fashion as the sum of kinetic parameters, represented as currents. The total current across a conductive polymer/liquid interface i_P can therefore be written as:

$$\frac{1}{i_P} = \frac{1}{i_T^c} + \frac{1}{i'_{ET}} + \frac{1}{i_{pol}} + \frac{1}{i''_{ET}} \qquad (1)$$

where i^c_T, i'_{ET}, i_{pol}, and i''_{ET}, represent, respectively, the tip current due to the diffusion of the redox mediator, the current due to the ET at the conductive polymer/liquid interface, the current due to charge transport across the polymeric film, and the current for ET at the polymer/metal interface. Because ET is fast at the underlying metal/conductive polymer interface, i''_{ET} is not rate-determining in the overall process and can be considered negligible. Contributions for the ET process can be divided into two categories: the diffusion-controlled redox mediator generation ($1/i^c_T$) and the ET across the polymeric film ($1/i'_{ET} + 1/i_{pol}$). Diffusive control is obtained for very thin polymeric films or for a low concentration of redox mediator. On the other hand, a thicker film and a high concentration of redox couples will lead to charge-transfer control. In the present case, the ET at the polymer/electrolyte interface depends primarily on the conductivity of the film. The SECM technique allowed an accurate determination of a heterogeneous rate constant, k_{eff}, because of the high sensitivity of feedback current to the rate of heterogeneous reactions.[33] From the SECM feedback current-distance curves, it is possible to extract a first-order effective heterogeneous constant by fitting the experimental results with the analytical approximation found for these processes.[24,34] The dependence of k_{eff} on the potential applied to the BBB and BBL films is strictly correlated to the conductivity properties of the film. When films are in the more conductive forms, the k_{eff} values are relatively high compared with the k_{eff} values when the film is not conductive (see Figure 6). These values can be represented as characteristic currents, i_{eff}, with the equation

$$i_{eff} = nFAC_M k_{eff} \qquad (2)$$

where C_M is the concentration of monomer ($7 \cdot 10^{-3}$ mol/cm^3 for the BBB and $8 \cdot 10^{-3}$ mol/cm^3 for the BBL) and A is the area below the tip ($5 \cdot 10^{-6}$ cm^2). This yields i_{eff} values in the conducting and resistive regimes ranging from $1.7 \cdot 10^{-5}$ to $2.4 \cdot 10^{-4}$ A for the BBL and from $1.7 \cdot 10^{-5}$ to $2.8 \cdot 10^{-4}$ for the BBB. These ratios are somewhat smaller than those predicted from the resistivities, assuming that the rds is charge transfer through the polymer.[22] However, as already shown, the film in its resistive form is somewhat permeable to diffusion of tip-generated species, and this contributes to the feedback current.

Comparison of resistance measurements (Figure 8) and the feedback current recorded at the tip close to the surface (Figures 2b and 3b) is of particular interest. Both measurements suggest an order-of-magnitude change in the film conductivities during the potential scan. In particular, the BBB film showed dramatic changes in the resistance properties during the first peak, whereas for the BBL film these changes occurred in the pre-peak zone. Furthermore, there were no appreciable changes in the film conductivity after the initial reduction, where the films changed their electronic state during the potential scan. The results suggest that electrochemical doping with compensation by electrolyte from the solution induces the greatest change in film conductivity. Furthermore, these results are consistent with previous ones,[13b,20a] where films were doped both electrochemically and chemically. The changes in the resistance could be caused by the electrochemical charging during the potential scan that produces gradients in concentrations of occupied (reduced) electron sites in the polymer. Such concentration polarization can by itself provide the driving force for the intersite electron hopping, whose rate can be qualitatively measured by the SECM feedback current or by resistance measurements.

Multistep chronoamperometry of BBL and BBB films (not shown) revealed a very stable and reversible electrochemical behavior under anaerobic and anhydrous conditions, and even after numerous reduction/oxidation cycles, the polymers continued to exhibit strong color changes in MeCN. The polymers in the neutral form were stable in air for at least 2 months.

Conclusion

BBB and BBL films spin-coated on ITO electrodes show interesting properties, including brilliant changes in film color and in resistance with the varying potential of the working electrode. Film characterization was performed by electrochemical, SECM, AFM, and resistance measurements. These conjugated ladder and

(30) Bard, A. J.; Fan, F.-R. F.; Mirkin, M. V. In *Electroanalytical Chemistry*; Bard, A. J., Ed.; Marcel Dekker: New York, 1994; Vol. 18, p 243.

(31) Wei, C.; Bard, A. J.; Mirkin M. V. *J. Phys. Chem.* **1995**, *99*, 16033.

(32) Tsionsky, M.; Bard, A. J.; Mirkin, M. V. *J. Am. Chem. Soc.* **1997**, *119*, 10785.

(33) Hubbard, A. T.; Anson, F. C. In *Electroanalytical Chemistry*; Bard, A. J., Ed.; Marcel Dekker: New York, 1970; Vol. 4, p 129.

(34) Tsionsky, M.; Bard, A. J.; Mirkin, M. V. *J. Phys. Chem.* **1996**, *100*, 17881.

semiladder polymers constitute an interesting class of electrochromic and electron transport materials.

Acknowledgment. This report is based on work supported by the U.S. Army Research Office under grant DAAD 19-99-1-0206. The support of this research by the Robert A. Welch Foundation is gratefully acknowledged. We thank Prof. Milena Koudelka for providing the microband device and Dr. Jian Wang for the AFM measurements.

CM001426F